Eur. Cytokine Netw. Vol. 36, n° 3 , *September 2025* 52-63

RESEARCH ARTICLE

Astilbin ameliorates propranolol-induced psoriasis-like lesions through restoring Th17/Treg immune homeostasis in lymph nodes

Yayun Wu[1,2,3#], Qi Xia[1#], Dancai Fan[1], Ya Zhao[1,3], Lijuan Liu[1,3], Shigui Deng[1,3], Ruizhi Zhao[1,2,3]

[1] The Second Clinical College of Guangzhou University of Chinese Medicine, Guangzhou University of Chinese Medicine, Guangzhou, China
[2] Guangdong Provincial Key Laboratory of Clinical Research on Traditional Chinese Medicine Syndrome, The Second Affiliated Hospital of Guangzhou University of Chinese Medicine, Guangzhou, China
[3] State Key Laboratory of Dampness Syndrome of Chinese Medicine, The Second Affiliated Hospital of Guangzhou University of Chinese Medicine, Guangzhou, China
[#] These authors contributed equally to this work.

Correspondence: R. Zhao
<13610241754@163.com>

Article accepted on 23 January 2026

To cite this article: Wu Y, Xia Q, Fan D, Zhao Y, Liu L, Deng S, Zhao R. Astilbin ameliorates propranolol-induced psoriasis-like lesions through restoring Th17/Treg immune homeostasis in lymph nodes. Eur. Cytokine Netw. 2025; 36(3): 52-63. doi: 10.1684/ecn.2025.0505

ABSTRACT. *Background*: Psoriasis is a challenging immune-mediated dermatological disorder with an urgent need for effective clinical therapeutics, while astilbin has shown considerable efficacy in suppressing psoriasis progression, its underlying mechanisms are not fully clarified. This study aimed to systematically investigate the anti-psoriatic effects of astilbin and to elucidate its potential mechanisms of action. *Methods:* A psoriasis-like mouse model was established via cold water swimming, dietary restriction, and topical application of 5% propranolol emulsion, followed by daily treatment with low- (25.6 mg/kg), middle- (51.2 mg/kg), or high-dose (76.8 mg/kg) astilbin for 6 consecutive days, with evaluations including PASI scoring, histopathological examination, Baker scoring, inflammatory cytokine detection, and flow cytometric analysis of lymphocyte populations in lymph nodes and spleen. *Results:* Middle and high doses of astilbin significantly reduced skin lesions and erythema, with PASI scores decreasing by 23.6%, and 44.9% respectively, Baker scores significantly reduced by 23.1% and 24.1% in the middle- and high-dose groups, and astilbin also significantly suppressed skin IL-17A, IL-6, and IFN-γ levels; moreover, middle and high doses substantially downregulated Th1, Th17, and Treg cell populations in lymph nodes and effectively restored Th17/Treg balance. *Conclusions:* Astilbin effectively ameliorates psoriatic skin lesions through immunomodulatory mechanisms involving the correction of lymph node Th17/Treg imbalance, highlighting its potential as a therapeutic agent for psoriasis.

Key words: psoriasis; astilbin; Th17/Treg; lymph nodes; propranolol

Psoriasis-like dermatitis constitutes a chronic immune-mediated inflammatory condition that predominantly affects the skin, nails, and joints [1, 2]. The global population of psoriasis patients almost doubled between 1990 and 2021, reaching 43 million, while 5.1 million new diagnoses were recorded in 2021 [3, 4]. The pathological hallmarks of psoriasis include epidermal hyperproliferation, dilation of dermal vascular networks, and pronounced inflammatory cell infiltration [5]. Contemporary research indicates that psoriasis pathogenesis involves complex interactions between genetic predisposition and environmental triggers, creating a multifactorial disease landscape.

As a prototypical autoimmune disorder, psoriasis pathophysiology encompasses the activation of diverse lymphocyte populations, including T helper 1 (Th1), T helper 17 (Th17), and regulatory T (Treg) cells. Th17 cells represent an activated T-cell subset that mediates inflammatory and autoimmune responses, while Treg cells function to maintain immune tolerance and prevent spontaneous autoimmune reactions [6, 7]. Accumulating evidence substantiates that the equilibrium between Th17 and Treg cells plays a pivotal role in the pathogenic mechanisms underlying various autoimmune conditions [8]. Consequently, maintaining an appropriate Th17/Treg ratio is essential for preserving immune homeostasis. Clinical investigations have consistently demonstrated significantly elevated levels of Th17 cells and their associated inflammatory mediators, including IL-6, IL-17, and IL-23 [9-13], in the serum of psoriatic patients. Concurrently, diminished expression of Treg cells and their regulatory cytokine TGF-β has been observed in psoriatic sera, collectively indicating a pronounced Th17/Treg imbalance in this condition [14, 15]. Furthermore, this immunological dysregulation promotes additional T-cell activation [16, 17] and facilitates the infiltration of inflammatory cells into the superficial dermis and epidermis. These events subsequently stimulate increased IFN-γ expression, thereby inducing

doi: 10.1684/ecn.2025.0505

keratinocyte proliferation and exacerbating psoriatic symptomatology [18]. Accordingly, therapeutic strategies aimed at rebalancing the Th17/Treg axis may offer promising approaches for mitigating psoriatic skin manifestations.

Current clinical management of psoriasis predominantly relies on immunosuppressive agents, including corticosteroids, vitamin D analogs, calcipotriol, and methotrexate [19, 20]. Although these pharmacological interventions can achieve satisfactory short-term therapeutic outcomes, their long-term utility is frequently compromised by adverse effects and the development of drug resistance [21]. Consequently, the discovery and development of safer anti-psoriatic agents with reduced side effect profiles represents a crucial objective in psoriasis therapeutics.

In recent years, traditional Chinese medicine and its principal active constituents have shown considerable promise in managing psoriasis. Astilbin, a dihydroflavonol glycoside, is widely distributed in edible Chinese herbal medicines such as Rhizoma smilacis glabrae [22] and Sarcandra glabra [23], as well as in common food sources including grapes and wine [24]. Substantial research has confirmed that astilbin possesses diverse biological activities encompassing immunomodulatory, antioxidant, anti-inflammatory, and anticancer properties [25]. Although studies demonstrate astilbin alleviates psoriasis by reducing reactive oxygen species [26], suppression of IL-6 and IL-22 expression [27], and inhibiting Th17 activation [28-30], its overall immunoregulatory mechanism remains poorly defined, limiting further therapeutic development. Notably, psoriasis onset and flares are frequently associated with psychological stress and metabolic disturbances, which can induce transient immunosuppression through dysregulation of the hypothalamic-pituitary-adrenal axis and sympathetic nervous system [31]. This hypoimmune state may paradoxically precede or exacerbate inflammatory episodes in susceptible individuals [32]. Clinically, many patients, especially after prolonged use of biologics, cyclosporine, or methotrexate, exhibit similar immune compromise. However, whether and how astilbin modulates psoriatic inflammation under such a hypoimmune background remains unexplored. Therefore, to better simulate this common clinical scenario and evaluate the immunomodulatory potential of astilbin in a more translationally relevant context, we established a novel psoriasis model combining chronic stress and metabolic preconditioning before propranolol-induced lesion formation.

METHOD AND MATERIALS

Drugs and reagents

Propranolol (purity ≥80%) was procured from Hubei Maiyuan Chemical Co., Ltd (Hubei, China). Astilbin (purity ≥95%) was obtained from Chengdu Purui Technology Co., Ltd (Chengdu, China) and subjected to HPLC analysis (*figure 1A*) following established

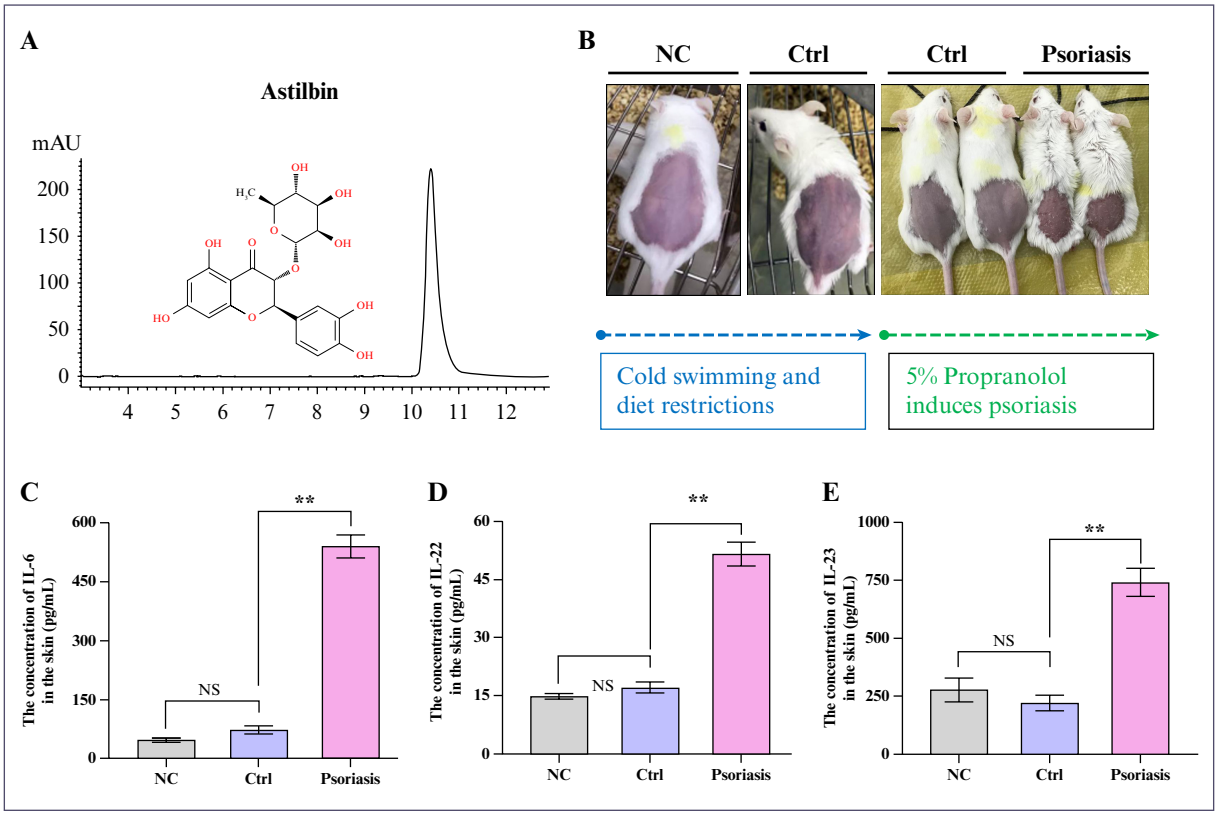

Figure 1

Astilbin identification and characterization of immunocompromised animal model. **(A)** Representative HPLC chromatogram of astilbin standard; **(B)** Schematic representation of immunocompromised model establishment; **(C)** Skin concentration of IL-6; **(D)** Skin concentration of IL-22; **(E)** Skin concentration of IL-23. Data presented as Mean ± SEM; NS indicates no statistical significance; $^{**}P<0.01$ versus control group. NC: Normal control group; Ctrl: Model control without propranolol; HPLC: High-performance liquid chromatography; IL-6: Interleukin-6; IL-22: Interleukin-22; IL-23: Interleukin-23; SEM: Standard error of the mean.

methodological protocols from previous research [33]. Methotrexate was purchased from Shanghai Xinyi Pharmaceutical Co., Ltd (Shanghai, China). Pentobarbital sodium was acquired from Sinopharm Group Rongsheng Pharmaceutical Co., Ltd. (Jiaozuo, China). The BCA protein quantification kit was procured from Thermo Scientific (MA, USA). Enzyme-linked immunosorbent assay (ELISA) kits for interleukin-6 (IL-6), IL-22, IL-23, and IL-17A were obtained from RayBio Co., Ltd (Georgia, USA). The interferon-gamma (IFN-γ) ELISA kit was purchased from Wuhan Huamei, Co., Ltd (Wuhan, China). Red blood cell lysate, PerCP-CY5.5 conjugated anti-mouse CD3e antibody, transcription factor buffer set, phycoerythrin (PE)-conjugated anti-mouse TNF-γ antibody, Alexa Fluor 647-conjugated anti-mouse IL-17A antibody, Alexa Fluor 647-conjugated anti-mouse CD4 antibody, allophycocyanin (APC)-conjugated anti-mouse CD25 antibody, PE-conjugated anti-mouse Foxp3 monoclonal antibody, and Leukocyte Activation Cocktail (with GolgiPlug) were all sourced from BD Biosciences (California, USA).

Animal experiments

Sixty specific-pathogen-free (SPF) grade Kunming mice (female, 25-30 g, 8 weeks old) were purchased from the Guangdong Medical Laboratory Animal Center (Guangdong, China) (certification No: SYXK Yue, 2013-0002). All animals were housed in SPF-controlled environments with ad libitum access to water and standard laboratory diet, maintained under a 12-hour light/dark cycle with controlled temperature (22±2 °C) and humidity (55±5%). All experimental procedures were conducted in strict accordance with the National Institutes of Health Guide for the Care and Use of Laboratory Animals and received approval from the Animal Ethics Committee of Guangzhou University of Chinese Medicine (Approval No. 2017024).

Following one week of acclimatization, mice were randomly allocated into two primary groups based on body weight: normal control group (n=10) and model group (n=50). Except for the normal control group, all remaining mice underwent daily swimming sessions in cold water (4 °C) for 5 minutes concurrently with dietary restriction to one-third of normal daily intake for 15 consecutive days to induce a hypoimmune state. Subsequently, 200 μL of 5% propranolol microemulsion, prepared in-house, was topically applied to the depilated dorsal skin region of model mice. The model mice were then randomly divided into five experimental groups (n=10 per group): model control group, astilbin low-dose group (25.6 mg/kg), astilbin middle-dose group (51.2 mg/kg), astilbin high-dose group (76.8 mg/kg), and positive control group (methotrexate, MTX, 3.792 mg/kg). The MTX dose was calculated via body surface area conversion (factor of 9.1) from the common human clinical dose (25 mg/week for a 70 kg adult), aligning with established protocols in murine psoriasis studies [34, 35]. Treatment compounds or equivalent volumes of 0.9% saline (for the normal and model control groups) were administered once daily via the appropriate route. On the sixth day of treatment, skin lesions were comprehensively evaluated according to the PASI scoring criteria detailed in *table 1*. Following assessment, all mice were humanely euthanized through deep anesthesia induced by intraperitoneal injection of pentobarbital sodium (80 mg/kg). Blood samples were collected via cardiac puncture, and dorsal skin tissues, spleens, and lymph nodes were carefully harvested. Skin specimens designated for histological analysis were immediately fixed in 4% paraformaldehyde solution. Serum samples, spleen tissues, and remaining skin samples were rapidly frozen and stored at -80 °C for subsequent biochemical and molecular analyses.

Determination of inflammation cytokines in the skin

The collected back skin tissues were thoroughly homogenized in RIPA lysis buffer at a weight/volume ratio of 1:10 using a mechanical homogenizer on ice. The homogenates were subsequently centrifuged at 12,000 × g for 15 minutes at 4 °C, and the resulting supernatants were collected for cytokine quantification. The concentrations of key inflammatory cytokines, including IL-6, IL-22, IL-23, IL-17A, IFN-γ, TNF-α, and TGF-β in skin tissues were precisely determined using commercially available ELISA kits according to the manufacturers' detailed protocols. Absorbance measurements were performed using a microplate reader, and cytokine concentrations were calculated based on appropriate standard curves generated for each assay.

Hematoxylin and eosin (H&E) staining and baker score

The collected skin tissues were fixed in 4% paraformaldehyde solution for 48 hours at room temperature, followed by sequential dehydration through graded ethanol series, clearing in xylene, and embedding in paraffin blocks. Tissue sections of 5 μm thickness were

Table 1.
PASI scoring criteria for skin lesions.

	Extent of skin lesions (Score)				
Items	**Asymptomatic**	**Mild**	**moderate**	**Severe**	**Extremely severe**
Erythema	0	1	2	3	4
Scaly	0	1	2	3	4
Thicken	0	1	2	3	4

PASI: Psoriasis Area and Severity Index.

prepared using a rotary microtome, mounted on glass slides, and subjected to standard H&E staining procedures. Briefly, sections were deparaffinized, rehydrated, stained with hematoxylin solution, differentiated, blued, counterstained with eosin, dehydrated, cleared, and mounted with neutral balsam. Pathological alterations in mouse skin sections were systematically examined and photo-documented under an upright optical microscope with 20× objective lens magnification. Baker scoring, a semi-quantitative histopathological assessment method, was performed by experienced pathologists blinded to experimental groups using photomicrographs obtained under 100× magnification according to the established criteria detailed in *table 2*. This scoring system evaluates multiple parameters, including hyperkeratosis, epidermal thickness, inflammatory cell infiltration, and dermal vascular changes.

Splenic lymphocytes determination in psoriatic mice

Splenic lymphocyte isolation was performed using mechanical dissociation and density gradient centrifugation. Briefly, 0.5 g of spleen tissue was gently ground on a 200-mesh stainless steel mesh, and splenocytes were eluted with cold PBS. The cell suspension was filtered through a 300-mesh nylon sieve to remove tissue debris and aggregates. The filtrate was centrifuged at 400 × g for 5 minutes at 4 °C to pellet cells. Erythrocyte contamination was eliminated by resuspending the cell pellet in 5 mL of red blood cell lysis buffer followed by incubation at 37 °C for 3 minutes. The lysis reaction was terminated by adding excess PBS, and cells were washed twice with cold PBS. After final centrifugation, viable lymphocytes were resuspended in 2 mL of RPMI-1640 medium supplemented with 10% heat-inactivated fetal bovine serum.

For flow cytometric analysis, 1×10^6 splenic lymphocytes were transferred to sterile centrifuge tubes and incubated with 2 μL of Fc receptor blocking solution at 4 °C for 5 minutes to prevent nonspecific antibody binding. For Treg cell characterization, surface staining was performed using PerCP-Cy5.5-conjugated anti-mouse CD3e, FITC-conjugated anti-mouse CD4, and APC-conjugated anti-mouse CD25 antibodies. All samples were incubated with antibody cocktails for 30 minutes at 4 °C in the dark. Following incubation, cells were washed twice with PBS, centrifuged at 4 °C for 5 minutes, and supernatants were carefully removed. Cell pellets were resuspended in 400 μL of 4% paraformaldehyde fixative solution and stored at 4 °C pending flow cytometric analysis. For intracellular Foxp3 staining, fixed cells were permeabilized with 1 mL of permeabilization buffer at 4 °C for 50 minutes, followed by incubation with PE-conjugated anti-mouse Foxp3 monoclonal antibody at 4 °C for 40 minutes. Cells were subsequently washed with 500 μL permeabilization buffer and resuspended in 400 μL of 4% paraformaldehyde. Treg cell subsets in the spleen were analyzed using a BD FACS Calibur flow cytometer (BD Biosciences, USA). Th1 and Th17 cells in splenic preparations were processed according to the pretreatment methodologies established for lymph node specimens, as comprehensively described in section 2.6.

Table 2 .
The Baker scoring criteria of skin pathology.

	Extent of skin lesions (Score)			
Items	**Mild**	**Moderate**	**Severe**	**Extremely severe**
Degree of tortuous basal layer	0.5	1	1.5	2
Inflammatory cell infiltration	0.5	1	1.5	2
Mastoid protrusion score	—	0.5	1	—
Telangiectasia score	—	0.5	—	—

Determination of Th1, Th17, and Treg cells in lymph nodes

Lymphocyte isolation from lymph nodes was performed using mechanical dissociation. Briefly, freshly harvested lymph nodes were placed in sterile Petri dishes containing cold PBS and gently ground using the plunger of a syringe. The resulting cell suspension was collected and passed through a cell strainer to remove tissue fragments. The filtrate was centrifuged at 400 × g for 5 minutes at 4 °C to pellet cells. The cell pellet was washed twice with PBS and resuspended in 1 mL of RPMI-1640 culture medium supplemented with 10% fetal bovine serum.

For Th1 and Th17 cell analysis, 1×10^6 lymphocytes from each sample were transferred to 96-well plates and incubated at 37 °C in a 5% CO_2 atmosphere for 30 minutes. Cells were then stimulated with 2 μL of phorbol 12-myristate 13-acetate (PMA) and incubated for 6 hours at 37 °C to induce cytokine production. Following stimulation, cells were washed with PBS, centrifuged, and resuspended in fresh PBS. Fc receptor blocking solution was added and incubated at 4 °C for 30 minutes. Cells were subsequently washed with PBS, centrifuged, and resuspended in 100 μL of permeabilization buffer for 20 minutes. After two washes with permeabilization buffer and centrifugation for 5 minutes, intracellular staining was performed using antibodies specific for IFN-γ and IL-17A. Samples were incubated with antibodies at 4 °C for 40 minutes, followed by resuspension in 400 μL of 4% paraformaldehyde. Th17 and Th1 cell subsets in lymph nodes were quantified using flow cytometry. Treg cells in lymph nodes were processed according to the pretreatment protocols established for splenic samples, as detailed in section 2.5.

Statistical analysis

All experimental data in this study are presented as mean ± standard error of the mean (SEM). Statistical analyses were performed using SPSS statistical software version 19.0 (IBM Corporation, Armonk, NY, USA). For multiple group comparisons of data conforming to normal distribution and homogeneity of variance, one-way analysis of variance (ANOVA) was employed,

followed by appropriate post-hoc tests. Non-parametric tests were utilized for multiple group comparisons of data that violated assumptions of normal distribution or homogeneity of variance. Differences between group means were considered statistically significant when the P-value was less than 0.05.

RESULTS

Therapeutic effect of astilbin on psoriasis-like skin lesion mice

Initial investigations focused on characterizing the animal model with induced low immunity. Following cold stimulation and dietary restriction, animals exhibited noticeable darkening of skin coloration, with faint purple spots becoming visibly apparent (*figure 1B*). After six days of continuous topical application of 5% propranolol, back skin samples were collected and concentrations of IL-6, IL-22, and IL-23 in skin tissues were quantitatively measured. Results demonstrated that the cold stimulation and dietary restriction did not significantly elevate inflammatory markers. However, following stimulation with 5% propranolol, psoriasis-related inflammatory factors in experimental animals showed substantial increases compared to the normal control group (*figure 1C-E*, $P<0.01$), indicating that the hypoimmune state can predispose to severe psoriasis development. In this study, the skin of normal mice maintained smooth and flat morphology without evident thickening, erythema, or other pathological manifestations.

In contrast, the dorsal skin of psoriasis model mice exhibited pronounced thickening, redness, swelling, and characteristic erythema infiltration (*figure 2A*). Following astilbin administration, the middle- and high-dose groups demonstrated significant reductions in PASI scores by 23.6% and 44.9%, respectively, compared to the model control group (*figure 2B*, $P<0.05$). The middle- and high-dose astilbin also reduced erythema scores by 21.7% and 22.2%, respectively (*figure 2C*), although these changes did not reach statistical significance ($P>0.05$). Moreover, all astilbin treatment groups showed no significant difference in infiltration (*figure 2D*) but substantial reductions in scaling scores by 67.1%, 58.6%, and 61.9%, respectively (*figure 2E*, $P<0.05$ or $P<0.01$), demonstrating improvement comparable to the methotrexate positive control group. Collectively, these findings indicate that astilbin possesses promising therapeutic effects on psoriatic skin lesions.

Pathological changes in skin

To systematically investigate the reparative effects of astilbin on psoriatic skin lesions, a comprehensive histopathological examination using H&E staining was conducted, with results quantified using the Baker scoring. As shown in *figure 3A*, characteristic psoriatic features, including hyperkeratosis, epidermal hyperplasia, dermal papillary vasodilation, and perivascular inflammatory cell aggregation around superficial dermal blood vessels, were evident, confirming successful establishment of the psoriasis model. Baker scoring

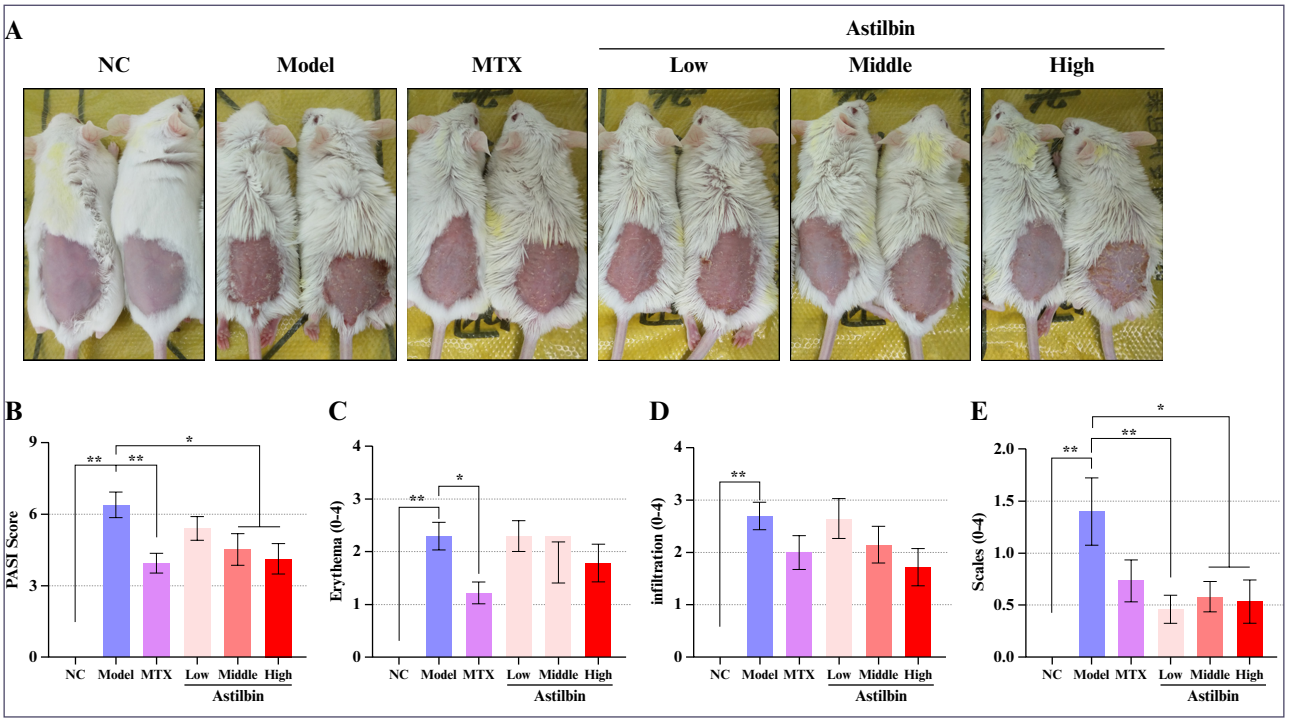

Figure 2
Astilbin ameliorates psoriasis-like skin lesions and reduces PASI scores in immunocompromised mice. **(A)** Representative photographic documentation of animal skin conditions across experimental groups; **(B)** Quantitative analysis of PASI scores; **(C)** Erythema severity scores; **(D)** Skin infiltration scores; **(E)** Scaling severity scores. Data presented as Mean ± SEM; *$P<0.05$, **$P<0.01$ versus model control group. NC: Normal control; MTX: Methotrexate; PASI: Psoriasis area and severity index; SEM: Standard error of the mean.

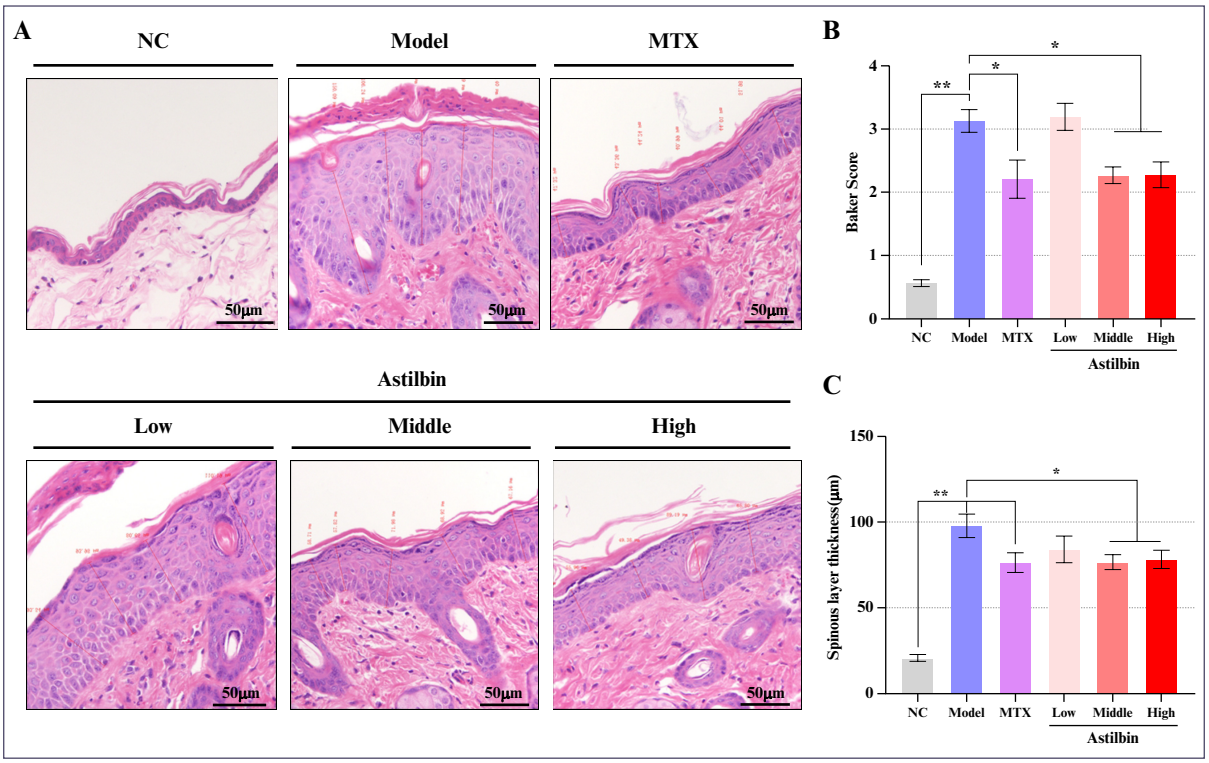

Figure 3

Therapeutic effects of astilbin on skin histopathology. **(A)** Representative photomicrographs of H&E stained back skin sections (200× magnification); **(B)** Quantitative analysis of Baker scores; **(C)** Measurement of spinous layer thickness. Data presented as Mean ± SEM; **P*<0.05, ***P*<0.01 versus model control group. NC: Normal control; MTX: Methotrexate; H&E: Hematoxylin and eosin; SEM: Standard error of the mean.

analysis revealed that methotrexate, high-dose astilbin, and middle-dose astilbin treatments significantly reduced Baker scores by 20.2%, 24.1%, and 23.1%, respectively, indicating substantial improvement in histopathological parameters (*figure 3B*). Particularly noteworthy, the high-dose astilbin group demonstrated significant inhibition of acanthosis (increased thickness of the spinous layer) (*figure 3C*), which may be mechanistically linked to the observed suppression of psoriatic skin erythema.

Astilbin inhibits inflammatory cytokines in the skin

Both gross morphological and histopathological observations confirmed that astilbin and methotrexate effectively ameliorate psoriasis-like skin lesions. To further elucidate the effects of astilbin on cutaneous inflammation, this study quantitatively determined inflammatory cytokine profiles in mouse skin tissues. Our results demonstrated that the concentration of IL-17A, IL-6, and IFN-γ were significantly elevated in skin lesions of the psoriasis model group (P<0.01). Astilbin administration substantially reduced the release of IL-17A and IFN-γ in skin lesions in a dose-dependent manner (*figure 4A, B*, *P*<0.05 or *P*<0.01). However, astilbin treatment did not exhibit significant regulatory effects on IL-6, TNF-α, and TGF-β levels in skin lesions (*figure 4C-E*). These findings suggest that suppression of IL-17A and IFN-γ may represent crucial mechanistic components in the anti-psoriatic activity of astilbin.

Astilbin reduces the cell proliferation of lymphocytes in lymph nodes

To investigate whether astilbin influences immune cell populations in lymphoid tissues, we quantitatively assessed the ratios of Th17 and Treg cells in lymph nodes. Following propranolol stimulation, significant activation of Th17 cells was observed in the psoriasis-like model (*figure 5A*). After intervention with the high, middle, and low-dose of astilbin, the proportion of activated Th17 cells was decreased by 45.4%, 51.9% (*P*<0.05), and 38.6%, respectively, compared with the model group (*figure 5B*).

Interestingly, propranolol induction also generated a significant increase in Treg cell numbers in lymph nodes (*figure 6A*). While Treg cells are typically downregulated in psoriasis, their induction under hypoimmune conditions resulted in upregulation. Middle and high doses of astilbin significantly decreased Treg cells by 26.6% and 22.8%, respectively, compared to the model group (*figure 6B*, *P*<0.01 or *P*<0.05).

To further characterize the comprehensive immune activation profile in lymph nodes, additional T-cell subsets including Th1, $CD3^+CD4^+$ T, and $CD4^+CD25^+$ T cells were evaluated. As shown in *figure 7A*, the proportion of Th1 cells in lymph nodes of propranolol-induced psoriatic animals increased significantly (*P*<0.01), and astilbin intervention substantially reduced Th1 cell populations (*P*<0.05 or *P*<0.01). However, the relative abundance of $CD3^+CD4^+$ T cells in lymph nodes remained unchanged following both modeling and

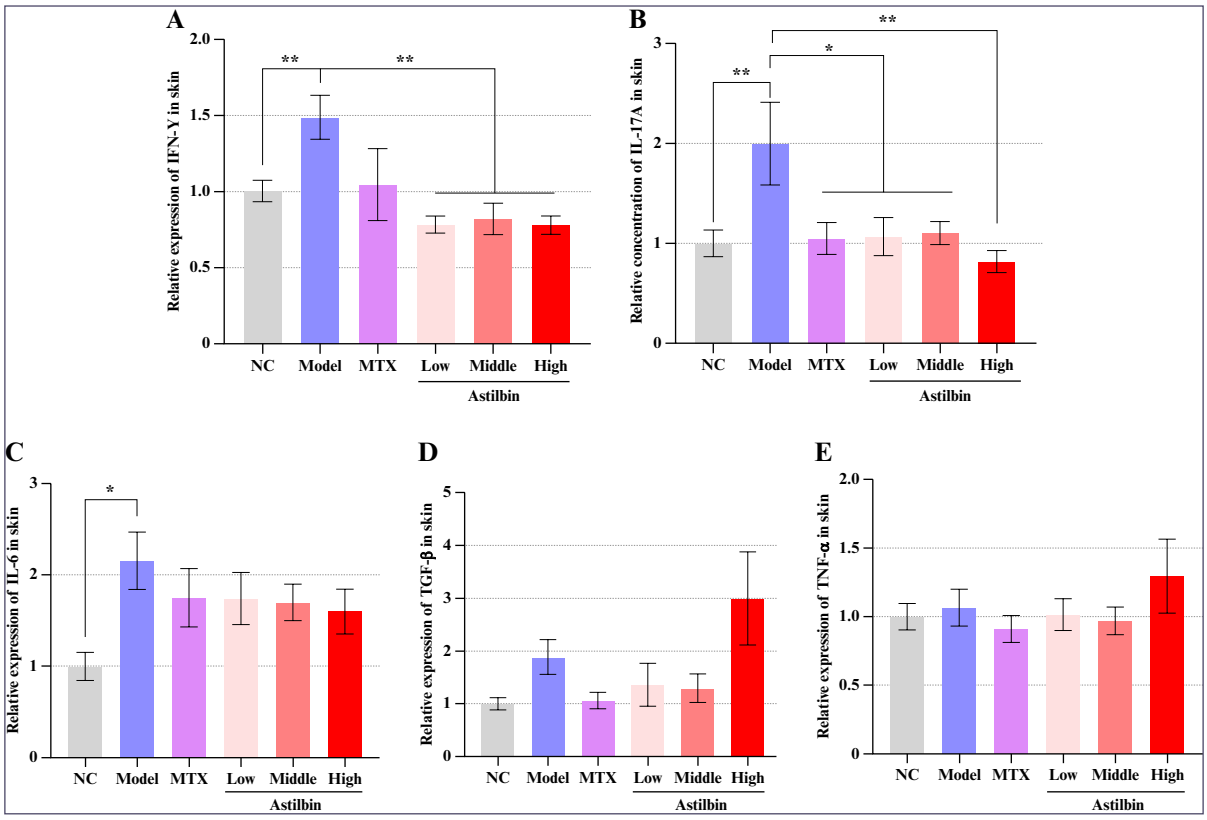

Figure 4
Modulatory effects of astilbin on inflammatory mediators in skin tissues. **(A)** IFN-γ concentration; **(B)** IL-17A concentration; **(C)** IL-6 concentration; **(D)** TGF-β concentration; **(E)** TNF-α concentration. Data presented as Mean ± SEM; **P*<0.05, ***P*<0.01 versus model control group. NC: Normal control; MTX: Methotrexate; IFN-γ: Interferon-gamma; IL-17A: Interleukin-17A; IL-6: Interleukin-6 TGF-β: Transforming growth factor-beta; TNF-α: Tumor necrosis factor-alpha; SEM: Standard error of the mean.

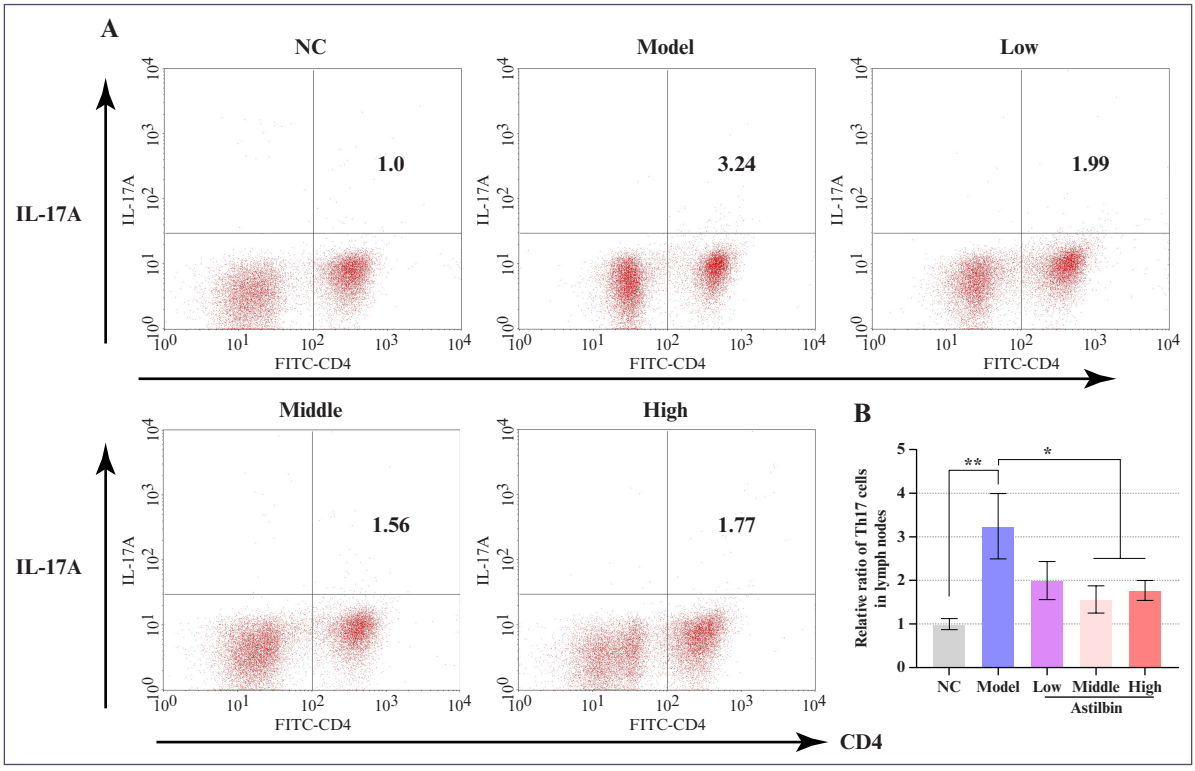

Figure 5
Effects of astilbin on Th17 cell proliferation in lymph nodes. **(A)** Representative flow cytometric plots of CD4+IL-17A+ cell populations; **(B)** Quantitative comparison of relative Th17 cell numbers in lymph nodes. Data presented as Mean ± SEM; **P*<0.05, ***P*<0.01 versus model control group. NC: Normal control; IL-17A: Interleukin-17A; CD4: Cluster of differentiation 4; Th17: T helper 17 cell; SEM: Standard error of the mean.

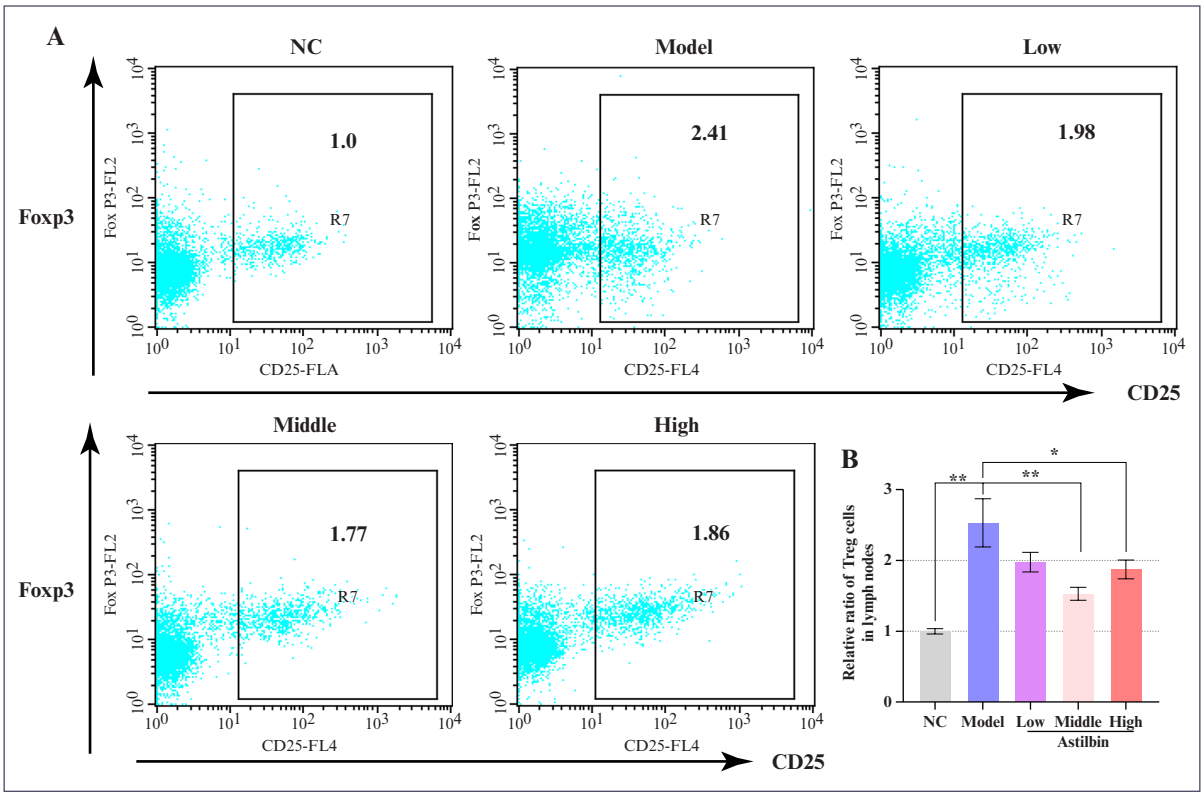

Figure 6
Effects of astilbin on Treg cell proliferation in lymph nodes. **(A)** Representative flow cytometric plots of CD25+Foxp3+ cell populations; **(B)** Quantitative comparison of relative Treg cell numbers in lymph nodes. Data presented as Mean ± SEM; *P<0.05, **P<0.01 versus model control group. NC: Normal control; Foxp3: Forkhead box P3; CD25: Cluster of differentiation 25; SEM: Standard error of the mean.

astilbin intervention (*figure 7B*). Additionally, compared to the normal control group, the proportion of $CD4^+CD25^+$ T cells increased dramatically after modeling (P<0.01), but only the middle-dose astilbin group significantly reduced $CD4^+CD25^+$ T cell numbers following intervention (*figure 7C*, P<0.01). Most importantly, the critical Th17/Treg ratio in lymph nodes showed significant increase following propranolol induction, indicating disruption of immune homeostasis. The high-dose astilbin group significantly downregulated the Th17/Treg ratio, suggesting that astilbin possesses substantial potential for restoring immune balance (*figure 7D*, P<0.05). These collective findings indicate that the anti-inflammatory effects of astilbin may be mechanistically linked to inhibition of Th1 cell proliferation and restoration of Th17/Treg balance in lymph nodes.

The effect of astilbin on lymphocytes in the spleen of psoriasis-like mice

To further explore the immunological mechanisms of astilbin, we analyzed psoriasis-associated lymphocyte populations in the spleen. As shown in *figure S1*, although Th17 cells increased moderately following model establishment, astilbin did not demonstrate significant regulatory effects on splenic Th17 cells. Treg cells in the spleen were activated after modeling (P<0.01), but modulatory effects of astilbin on splenic Treg cells were minimal (*figure S2*). Furthermore, results indicated that Th1 and $CD3^+CD4^+$ T cell populations in the spleen remained unchanged following modeling, while $CD4^+CD25^+$ T cells increased significantly (*figure S3*, P<0.05). However, astilbin administration did not produce significant effects on these splenic immune cell populations.

DISCUSSION

Psoriasis is a chronic inflammatory dermatosis driven by complex interactions among keratinocytes, dendritic cells, and T lymphocytes [36], highlighting the central role of immunomodulation in its pathogenesis. Consequently, immunomodulation plays an essential role in both the initiation and progression of psoriatic pathology. The present study demonstrates that astilbin effectively alleviates psoriatic skin lesions in a novel animal model, as evidenced by reduced PASI and Baker scores, along with decreased secretion of IL-17A and IFN-γ in skin tissue and rebalancing Th17/Treg in the lymph nodes. These findings underscore the therapeutic potential of astilbin.

Psoriasis is conventionally considered an immune hyperactivation disorder, and numerous immunosuppressive agents, including methotrexate and cyclosporine A, are routinely employed in clinical management, yet clinical observations indicate that patients frequently exhibit a hypoimmune state during remission, which may predispose them to subsequent flares [37, 38]. These clinical observations suggest that immune compromise may represent a crucial factor in precipitating psoriasis onset and progression. In social contexts, low immunity often

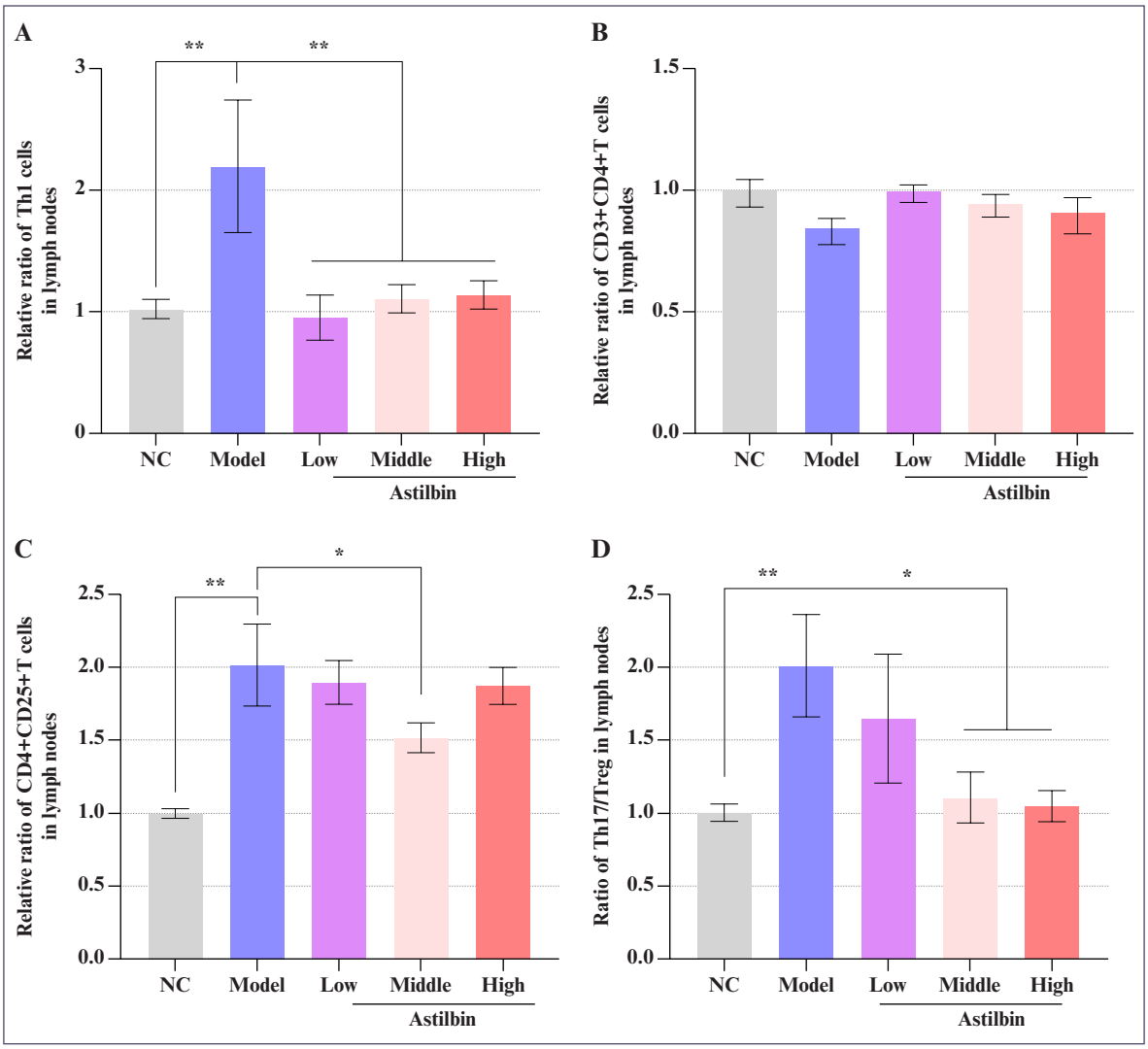

Figure 7
Comprehensive effects of astilbin on Th1, $CD3^+CD4^+$ T, and $CD4^+CD25^+$ T cell proliferation and Th17/Treg ratio in lymph nodes. **(A)** Quantitative analysis of relative Th1 cell numbers; **(B)** Quantitative analysis of relative CD3+CD4+ T cell numbers; **(C)** Quantitative analysis of relative $CD4^+CD25^+$ T cell numbers; (D) Th17/Treg ratio in lymph nodes. Data presented as Mean ± SEM; $*P<0.05$, $**P<0.01$ versus model control group. NC: Normal control; Th1: T helper 1 cell; Th17: T helper 17 cell; CD3: Cluster of differentiation 3; CD4: Cluster of differentiation 4; CD25: Cluster of differentiation 25; SEM: Standard error of the mean.

correlates with chronic malnutrition or insufficient energy intake [39]. Preliminary investigations have corroborated that reduced immune competence increases susceptibility to psoriasis induction under conditions of cold stress [40, 41] and dietary restriction [42]. To investigate the pathogenesis and therapeutic strategies under this clinically relevant condition, we established a composite model that combines chronic cold stress and dietary restriction to induce a systemic hypoimmune state, with topical propranolol administration serving as a "second hit" to trigger psoriasis. Unlike the acute, IL-23/Th17-centered response driven by imiquimod (IMQ) via TLR7/8 [10, 43], our model mimics the dynamic interplay between systemic immune compromise and localized inflammation triggered by common stressors, providing a complementary tool for etiological and therapeutic research.

Treg cells are essential for maintaining immunological homeostasis [44]. Further immunophenotyping revealed that astilbin downregulated propranolol-induced activation of Th1, Th17, and Treg cells in lymph nodes of this model. This is consistent with previous reports that astilbin modulates T-cell differentiation and function, including enhancing Treg activity and inhibiting Th17 polarization [45, 46]. This coordinated downregulation of key pathogenic axes alongside regulatory T cells suggests a multi-target mechanism. It aligns with reports that astilbin inhibits pivotal signaling pathways like JAK/STAT3 and NF-κB [47], and extends previous findings by demonstrating integrated regulation of the Th1/Th17/Treg network in vivo under stress conditions. Such broad modulation of the Th1/Th17/Treg network positions astilbin not merely as a selective inhibitor but as a regulator of immune homeostasis, capable of attenuating the synergistic inflammation characteristic of psoriasis. Although a downward trend in skin IL-6 expression was observed, this trend lacked statistical significance. This may be attributed to sampling timing or experimental variability, yet the consistent suppression of key effector cytokines supports its functional

impact. Overall, astilbin appears to exert its anti-psoriatic effect through a pluralistic immunoregulatory approach, underscoring its potential as a multi-target therapeutic agent.

Moreover, two model-related observations warrant further discussion. First, an increase in Treg numbers was observed, contrasting with some clinical reports in chronic psoriasis. This is consistent with findings in acute murine models like IMQ-induced psoriasis, where a transient compensatory rise in Tregs occurs during active inflammation [48]. This highlights that the critical defect may be the functional insufficiency of Tregs against an overwhelming Th17 response, a balance effectively restored by astilbin. Second, the effects of astilbin were pronounced in lymph nodes but minimal in the spleen. This differential response is compounded by pharmacokinetics: distribution studies indicate that astilbin achieves relatively low exposure in the spleen compared to other organs [49], while in our model, lymph nodes, as draining sites receiving both systemic stress and local propranolol signals, contain T cells in a highly activated state [50, 51], making them more susceptible to the modulatory effects of astilbin.

Furthermore, our study demonstrated that astilbin did not significantly affect $CD3^+CD4^+$ T cell populations in lymph nodes, suggesting that propranolol-induced skin lesions primarily represent localized inflammatory responses with minimal impact on $CD4^+$ T cell dynamics. This observation also implies that astilbin may exert negligible effects on systemic immunity. Conversely, the effects of astilbin on $CD4^+CD25^+$ T cells paralleled its regulation of Treg cells. The reduction in pro-inflammatory Th17 cells exceeded that of total Treg cells, confirming that astilbin specifically modulates immune balance in lymph nodes.

In summary, astilbin ameliorates psoriasis-like inflammation in a stress-precipitated model through pluralistic immunoregulation, primarily targeting the dysregulated Th1/Th17/Treg axis in draining lymph nodes. Our findings support its potential as a multi-target therapeutic agent. Future studies should directly assess the functional capacity of Tregs in this context, investigate formulation strategies to overcome pharmacokinetic limitations for systemic effects, and further elucidate the precise molecular targets of astilbin within the immune network.

Limitations

In this study, we only examined the number and proportion of cells at specific time points, but failed to directly evaluate the suppressive function of the expanded Treg cells in the model. This limitation constrains the understanding of the depth of immune homeostasis restoration. Secondly, the pharmacological effects of astilbin exhibit marked tissue specificity, which is partially consistent with its pharmacokinetic distribution characteristics. However, this study did not directly determine the actual concentration of astilbin in different lymphoid organs; thus, the evidence for the mechanism underlying its tissue selectivity remains indirect inference. Furthermore, the established combined stress model was designed to simulate the clinically common pathogenic scenario induced by hypoimmune status, yet its correlation with the pathological progression of specific clinical subtypes of psoriasis requires further validation and confirmation through additional preclinical and clinical studies.

CONCLUSION

This study demonstrates that astilbin effectively ameliorates psoriatic lesions in a novel stress-induced hypoimmune model. Its therapeutic mechanism involves the coordinated downregulation of pathogenic Th1 and Th17 responses alongside the modulation of Treg cells in lymph nodes, thereby restoring the critical Th17/Treg balance and showcasing multi-target immunomodulatory properties. These findings highlight the potential of astilbin as a promising therapeutic agent that acts by rebalancing immune homeostasis.

DISCLOSURE

Financial support: This work was partially supported by the project of the Guangdong Province Hospital of Traditional Chinese Medicine (Grant no. YN2019MJ06). The project of the State Administration of Traditional Chinese Medicine Clinical Base Fund (Grant No. JDZX2015206).

Ethics Approval: All animal experiments were conducted in accordance with the NIH Guide for the Care and Use of Laboratory Animals and approved by the Animal Ethics Committee of Guangzhou University of Chinese Medicine (Approval No. 2017024).

Author Contributions: Yayun Wu and Qi Xia performed experiments and wrote the manuscript; Lijuan Liu and Dancai Fan participated in some experiments and analyzed the data; Yayun Wu, Ya Zhao, and Shigui Deng contributed to the original idea and carefully revised the manuscript. Ruizhi Zhao: Supervised, designed, and edited the manuscript.

Availability of Data and Materials: The data supporting the conclusions of this article are included within the article and its supplementary materials. Additional raw data are available from the corresponding author Ruizhi Zhao (E-mail: zhaoruizhi@gzucm.edu.cn) upon reasonable request.

Conflict of Interest: The authors confirm that they have no conflicts of interest in the work described in this manuscript.

REFERENCES

1. Xia T, Zhang W, Wu R, *et al.* Dermal adipogenesis protects against neutrophilic skin inflammation during psoriasis pathogenesis. *Cell Mol Immunol* 2025;22:901-17.
2. Lee JYW, Mahil SK. Systemic inflammation and psoriasis: unpicking a complex relationship. *Br J Dermatol* 2025;2:2.
3. Xiong J, Xue T, Tong M, *et al.* Dynamic trend analysis of global psoriasis burden from 1990 to 2021: a study of gender, age, and regional differences based on GBD 2021 data. *Front Public Health* 2025;13:1518681.
4. Wei J, Wang Y, Chen Y, *et al.* Global burden of psoriasis from 1990 to 2021 and potential factors: a systematic analysis. *J Invest Dermatol* 2025.

5. Xia L, Li H, Long L, *et al.* Research progress on the pathogenesis of psoriasis and its small molecule inhibitors. *Arch Pharm (Weinheim)* 2025;358:e2400621.
6. Potestio L, Martora F, Lauletta G, *et al.* The role of interleukin 23/17 axis in psoriasis management: a comprehensive review of clinical trials. *Clin Cosmet Investig Dermatol* 2024;17:829-42.
7. Graßhoff H, Comdühr S, Nording H, *et al.* Transition from psoriasis to psoriatic arthritis is characterized by distinct alterations in peripheral blood Tc17, Th17, and CD4(+) effector memory cells. *Arthritis Rheumatol* 2025:1-10.
8. Hu Y, Zhao Q, Dai H, *et al.* Metabolic reprogramming as a therapeutic target for modulating the Th17/Treg balance in autoimmune diseases: a comprehensive review. *Front Immunol* 2025;16:1687755.
9. Jones SA, Perera DN, Fan H, *et al.* GILZ regulates Th17 responses and restrains IL-17-mediated skin inflammation. *J Autoimmun* 2015;61:73-80.
10. Van D, Mourits S, Voerman J, *et al.* Imiquimod-induced psoriasis-like skin inflammation in mice is mediated via the IL-23/IL-17 axis. *J Immunol* 2009;182:5836.
11. Gryka-Marton M, Grabowska A, Szukiewicz D. Effect of proinflammatory cytokines on blood-brain barrier integrity. *Eur Cytokine Netw* 2024;35:38-47.
12. Alsabbagh MM. Cytokines in psoriasis: from pathogenesis to targeted therapy. *Hum Immunol* 2024;85:110814.
13. Van Damme J, Opdenakker G, Van Damme S, Struyf S. Antibodies as tools in cytokine discovery and usage for diagnosis and therapy of inflammatory diseases. *Eur Cytokine Netw* 2023;34:1-9.
14. Shi Y, Chen Z, Zhao Z, *et al.* IL-21 induces an imbalance of Th17/Treg cells in moderate-to-severe plaque psoriasis patients. *Front Immunol* 2019;10:1865.
15. Kanda N, Hoashi T, Saeki H. The defect in regulatory T cells in psoriasis and therapeutic approaches. *J Clin Med* 2021;10: 3880.
16. Lin Y, Li B, Xue K, Wang G. CDK7 inhibitor suppresses psoriasis inflammation via inhibiting glycolysis to modulate Th17/Treg balance. *J Invest Dermatol* 2020;140:S8.
17. Deng Y, Chang C, Lu Q. The inflammatory response in psoriasis: a comprehensive review. *Clin Rev Allergy Immunol* 2016;50:377-89.
18. Chang W, Liang N, Cao Y, *et al.* The effects of human dermal-derived mesenchymal stem cells on the keratinocyte proliferation and apoptosis in psoriasis. *Exp Dermatol* 2021;30:943-50.
19. Stanescu AMA, Simionescu AA, Diaconu CC. Oral vitamin D therapy in patients with psoriasis. *Nutrients* 2021;13:163-71.
20. Barrea L, Savanelli MC, Di Somma C, *et al.* Vitamin D and its role in psoriasis: an overview of the dermatologist and nutritionist. *Rev Endocr Metab Disord* 2017;18:1-11.
21. Subedi S, Gong Y, Chen Y, Shi Y. Infliximab and biosimilar infliximab in psoriasis: efficacy, loss of efficacy, and adverse events. *Drug Des Devel Ther* 2019;13:2491-502.
22. Lu CL, Zhu YF, Hu MM, *et al.* Optimization of astilbin extraction from the rhizome of *Smilax glabra*, and evaluation of its anti-inflammatory effect and probable underlying mechanism in lipopolysaccharide-induced RAW264.7 macrophages. *Molecules* 2015;20:625-44.
23. Zhao RZ, Zhao Y, Zhang LQ, Lu CJ. Determination of isofraxidin and astilbin by HPLC in rat plasma and its application after orally administration the extract of *Sarcandra glabra*. *Pak J Pharm Sci* 2013;26:1-6.
24. Yang D, Zhang QF. The natural source, physicochemical properties, biological activities and metabolism of astilbin. *Crit Rev Food Sci Nutr* 2023;63:9506-18.
25. Sun X, Zhang H, Zhang Y, *et al.* Caspase-dependent mitochondrial apoptotic pathway is involved in astilbin-mediated cytotoxicity in breast carcinoma cells. *Oncol Rep* 2018;40:2278-86.
26. Wang W, Yuhai, Wang H, *et al.* Astilbin reduces ROS accumulation and VEGF expression through Nrf2 in psoriasis-like skin disease. *Biol Res* 2019;52:49.
27. Yu J, Xiao Z, Zhao R, *et al.* Astilbin emulsion improves guinea pig lesions in a psoriasis-like model by suppressing IL-6 and IL-22 via p38 MAPK. *Mol Med Rep* 2018;17:3789-96.
28. Xu X, Zhang H, Chang A, *et al.* Astilbin alleviates IL-17-induced hyperproliferation and inflammation in HaCaT cells via inhibiting ferroptosis through the cGAS-STING pathway. *Int J Mol Sci* 2025;26: 5075.
29. Xia Q, Huang X, Li A, *et al.* OASL activates MAPK to drive psoriatic pathogenesis: astilbin targeting this axis improves metabolic-inflammation crosstalk. *Life Sci* 2025;375:123698.
30. Tang Y, Yu J, Zhao W, *et al.* Total glucosides of *Rhizoma Smilacis Glabrae*: a therapeutic approach for psoriasis by regulating Th17/Treg balance. *Chin J Nat Med* 2023;21:589-98.
31. Potestio L, Lauletta G, Tommasino N, *et al.* Risk factors for psoriasis flares: a narrative review. *Psoriasis Targets Ther* 2024;14:39-50.
32. Nunez SG, Rabelo SP, Subotic N, *et al.* Chronic stress and autoimmunity: the role of HPA axis and cortisol dysregulation. *Int J Mol Sci* 2025;26: 9994.
33. Zhang ZF, Lu LY, Liu Y, *et al.* Determination of antioxidants in *Smilacis Glabrae Rhizoma* by high-performance liquid chromatography with ultraviolet and mass spectrometry detection. *Anal Lett* 2016;49:1975-85.
34. Czarnecka-Operacz M, Sadowska-Przytocka A. The possibilities and principles of methotrexate treatment of psoriasis – the updated knowledge. *Postep Derm Alergol* 2014;31:392.
35. El-Esawy FM, Ahmed IA, El-Fallah AA, Salem RM. Methotrexate mechanism of action in plaque psoriasis: something new in the old view. *J Clin Aesthet Dermatol* 2022;15:42-6.
36. Albanesi C, Madonna S, Gisondi P, Girolomoni G. The interplay between keratinocytes and immune cells in the pathogenesis of psoriasis. *Front Immunol* 2018;9:1549-56.
37. Strober BE, Siu K, Menon K. Conventional systemic agents for psoriasis. A systematic review. *J Rheumatol* 2006;33:1442-6.
38. Zeng J, Tang Z, Zhang Y, *et al.* Ozonated autohemotherapy elevates PPAR-gamma expression in CD4(+) T cells and serum HDL-C levels, a potential immunomodulatory mechanism for treatment of psoriasis. *Am J Transl Res* 2021;13:349-59.
39. Kogut MH, Klasing K. An immunologist's perspective on nutrition, immunity, and infectious diseases: introduction and overview. *J Appl Poult Res* 2009;18:103-10.
40. Yang J, Li G, Yue L, *et al.* The impacts of seasonal factors on psoriasis. *Exp Dermatol* 2025;34:e70078.
41. Sun L, Wang X, Zou Y, *et al.* Cold stress induces colitis-like phenotypes in mice by altering gut microbiota and metabolites. *Front Microbiol* 2023;14:1134246.
42. Muzumdar S, Rothe MJ. Nutrition and psoriasis. *Clin Dermatol* 2022;40:128-34.
43. Chen WC, Wen CH, Wang M, *et al.* IL-23/IL-17 immune axis mediates the imiquimod-induced psoriatic inflammation by activating ACT1/TRAF6/TAK1/NF-κB pathway in macrophages and keratinocytes. *Kaohsiung J Med Sci* 2023;39:789-800.
44. Schwarz A, Philippsen R, Schwarz T. Induction of regulatory T cells and correction of cytokine disbalance by short-chain fatty acids: implications for psoriasis therapy. *J Invest Dermatol* 2021;141:95-104.

45. Meng QF, Zhang Z, Wang YJ, *et al.* Astilbin ameliorates experimental autoimmune myasthenia gravis by decreased Th17 cytokines and up-regulated T regulatory cells. *J Neuroimmunol* 2016;298:138-45.

46. Xu Q, Liu Z, Cao Z, *et al.* Topical astilbin ameliorates imiquimod-induced psoriasis-like skin lesions in SKH-1 mice via suppression dendritic cell-Th17 inflammation axis. *J Cell Mol Med* 2022;26:1281-92.

47. Feng H, Li C, Chen J, *et al.* Astilbin from *Smilax china* L. remarkably inhibits LPS-induced endometritis in rats via blocking positive feedback between TLR4 and IL-6R signalling pathways in a PPAR-γ-dependent manner. *J Ethnopharmacol* 2025;348:119861.

48. Chong WC, Bo RK, Yang S, *et al.* Regulatory T cells suppress skin inflammation in the imiquimod-induced psoriasis-like mouse model. *J Dermatol Sci* 2020;98: 199-202.

49. Shi M, Xu M, Yin L. Pharmacokinetic, bioavailability and tissue distribution study of astilbin in rats. *J Pharm Pharmacol* 2020;72:1061-71.

50. Guo LL, Liu W, Lu TT, *et al.* Decrease of functional activated T and B cells and treatment of glomerulonephritis in lupus-prone mice using a natural flavonoid astilbin. *PLoS One* 2015;10:e0124004.

51. Choe J, Nair M, Basha R, *et al.* Defining early life stress as a precursor for autoimmune disease. *Crit Rev Immunol* 2019;39:329-42.